The Capsule-Fill-Tube-Assembly Mapping System

N. A. Antipa

December 20, 2012

Disclaimer

This document was prepared as an account of work sponsored by an agency of the United States government. Neither the United States government nor Lawrence Livermore National Security, LLC, nor any of their employees makes any warranty, expressed or implied, or assumes any legal liability or responsibility for the accuracy, completeness, or usefulness of any information, apparatus, product, or process disclosed, or represents that its use would not infringe privately owned rights. Reference herein to any specific commercial product, process, or service by trade name, trademark, manufacturer, or otherwise does not necessarily constitute or imply its endorsement, recommendation, or favoring by the United States government or Lawrence Livermore National Security, LLC. The views and opinions of authors expressed herein do not necessarily state or reflect those of the United States government or Lawrence Livermore National Security, LLC, and shall not be used for advertising or product endorsement purposes.

Automated ICF Capsule Characterization Using Confocal Surface Profilometry

N. A. Antipa*, S. H. Baxamusa, E. S. Buice, A. D. Conder, M. N. Emerich, M. S. Flegel,
C. L. Heinbockel, J. B. Horner, J. E. Fair, L. M. Kegelmeyer, E. S. Koh, M. A. Johnson,
W. L. Maranville, J. S. Meyer, R. Montesanti, J. Nguyen, J. E. Ralph, J. L. Reynolds,
J. G. Senecal

1. Abstract

Capsule ablators are precision hollow spheres used in inertial confinement fusion (ICF) targets used in high-peak-power lasers systems such as the National Ignition Facility. These capsules have high surface quality requirements and hence a full surface microscopic mapping system has been developed to characterize them. The Capsule-Fill-Tube-Assembly (CFTA) mapping system combines a confocal surface-profiling microscope with a nine-axis high precision stage system in order to provide quantitative three-dimensional data over the entire surface of each capsule prior to assembly into the final target. The system measures the individual volumes of features on the capsule surface that are 7.5 μm^3 and larger with an accuracy of ± 10 percent. The positional accuracy is better than 0.25 degree (1σ), or approximately 5μm linearly. The data acquisition and image processing are all highly automated in order to keep pace with throughput demands. The system consists of four primary subsystems: the positioning system, the confocal microscope, the automated acquisition code, and the image processing and data management software.

2. Introduction

Isolated asperities on the surfaces of inertial confinement fusion (ICF) capsules can seed Rayleigh-Taylor instability during implosion, which leads to ablator material mixing with the hot core, cooling the core and reducing the probability of ignition [1]. In order to ensure stable capsule performance during ignition shots at the National Ignition Facility (NIF), the ablator surface must be free of foreign particles of volume greater than 30 μm^3. In addition, ignition quality capsules must have at most 10 particles with volumes between 15 and 30 μm^3, and fewer than 50 particles between 7.5 and 15 μm^3. These volume bins correspond to spheres of diameter 3.8 μm, 3.1 μm, and 2.4 μm, respectively.

This stringent cleanliness requirement demands a system that is capable of reliable three dimensional measurements of isolated features with volumes ≥7.5 μm^3. In order to maintain 10 percent measurement accuracy for volumes as small as 7.5 μm^3, measurement accuracy of less than 0.16 μm laterally, and 0.1 μm vertically are required.

3. Discussion

3.1 Metrology Method Selection

The key requirement of the CFTA mapping system is that it must be capable of three-dimensional measurement of any small contaminants on a capsule's surface. Particles can span a wide array of optical properties, so a robust surface profiling technique must be used.

The initial investigation into metrology methods capable of meeting the aforementioned accuracy requirements spanned both contact and non-contact profilometry, including Phase Shifting Interferometry (PSDI) [5], White Light Vertical Scanning Interferometry (VSI), Atomic Force Microscopy (AFM), and Surface Profiling Confocal Microscopy. Though AFM could easily meet the requirements, the scan times would be prohibitively long. That left PSDI, VSI, and confocal as the remaining options.

Due to its preexisting implementation in NIF capsule metrology and its nanometer vertical resolution, PSDI was the first technology investigated for the particle metrology task. Unfortunately, in early testing it became apparent that the phase measurements on small scattering particles were not reliable. Figure 1 shows an example of PSDI height measurements of a particle with lateral dimensions of 3μm x 5μm, and a height of approximately 0.5μm, compared to a scanning electron microscope (SEM) image of the same particle, acquired with an inclination angle of approximately 80 degrees to emphasize the height. Though the PSDI accurately measures the smooth spherical surface features, the line trace of the PSDI data shows that the particle was not accurately measured.

VSI also proved to be unusable on small, scattering particles, primarily due to dynamic range issues. Because scattering particles appear very dark compared to the highly specular capsule surface, the VSI system tested required imaging the particles on a steeply sloped region of the capsule in order to decrease the background intensity into a range where both the particle and the capsule surface could be measured. However, even after making this adjustment, the topographic data were found to contain many erroneous spikes and pits. Figure 1 shows a VSI image of the same particle shown in Figure 1, and clearly illustrates the types of flaws seen in VSI measurements of particles on capsule surfaces.

The final technology investigated was confocal surface profiling. Examining a number of small particles under the Leica DCM 3D confocal microscope and comparing to SEM, it became apparent that confocal surface profiling was the most adept at simultaneously measuring both very rough particles and very smooth capsule surfaces.
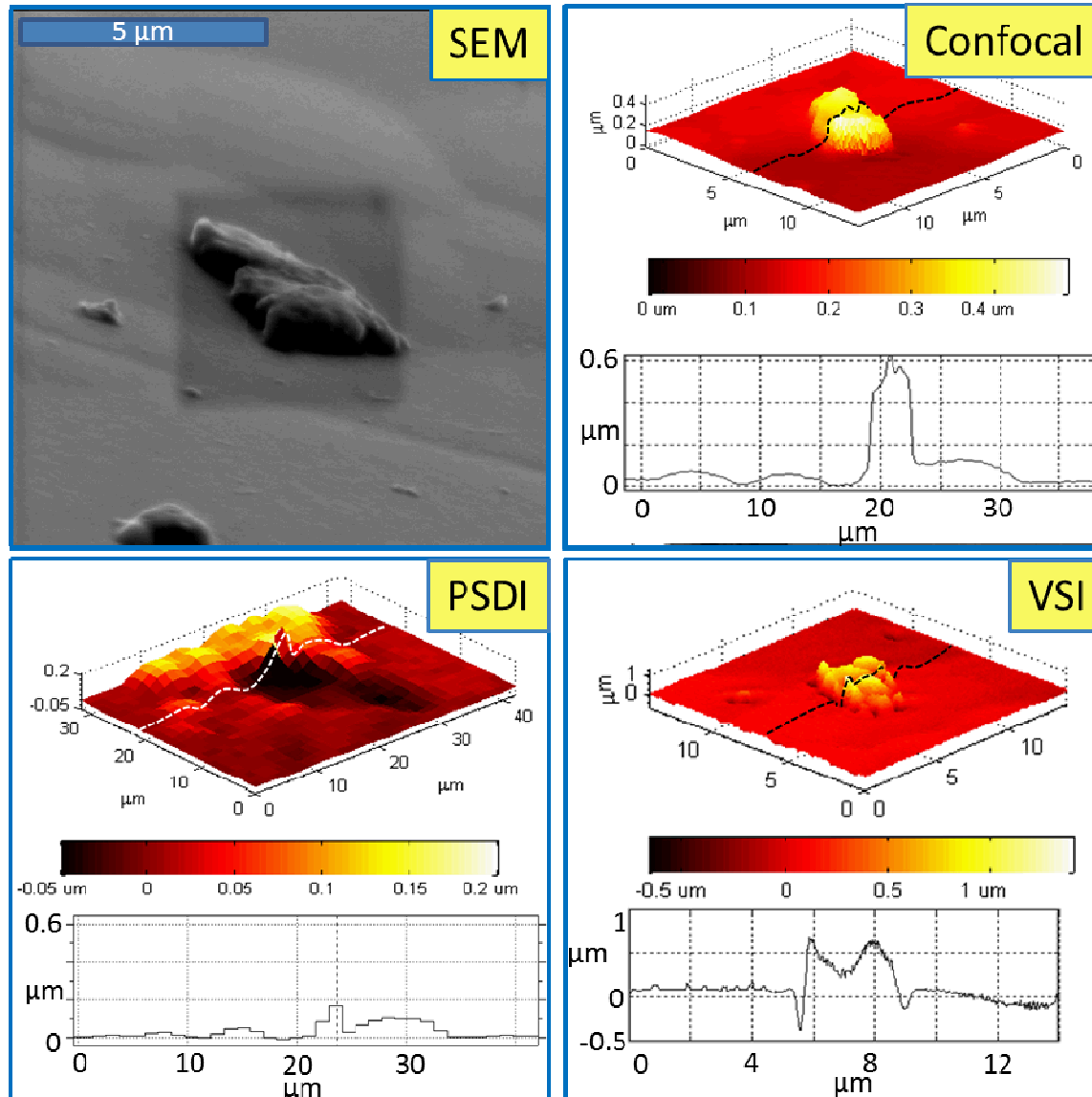
Figure 1. SEM (upper left) compared to confocal surface profiling (upper right), PSDI (lower left), and VSI (lower right). The SEM was image taken at 80 degree inclination to emphasize particle height. PSDI accurately measures spherical domes on capsule surface, but misses the particle altogether. VSI is rife with artificial pits and divots. The confocal method agrees best with the SEM.

3.2 Surface Profiling Confocal Microscopy

The defining characteristic of a confocal microscope is the presence of a spatial filter in the back focal plane of the optical system. This spatial filter is conjugate to the image plane— hence the name "confocal"—and consists of a single pinhole in the canonical confocal microscope design. This spatial filter rejects rays originating from outside the object plane, ensuring that only in-focus photons are collected. In a single pinhole setup, the intensity is only measured at one (X,Y) position at a time, necessitating scanning of either the pinhole in the back focal plane, or the sample in the object plane. Integrating the intensity as a

function of pinhole (or object) position produces an optical cross section of the sample in which only sample features falling within the depth of field (DOF) of the object plane appear illuminated in the image. Figure 2 shows a simulation of the annular shape of a single optical section from a spherical sample such as a NIF capsule.
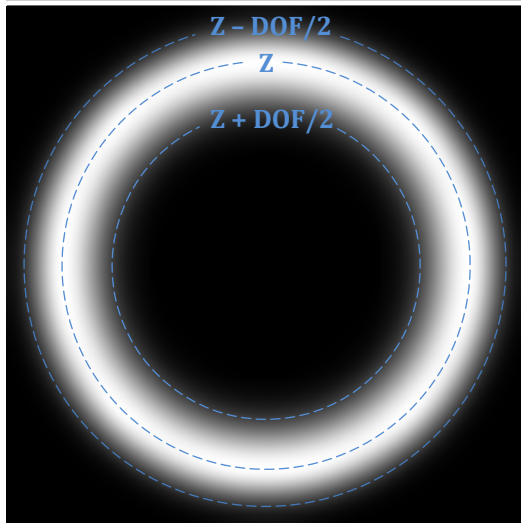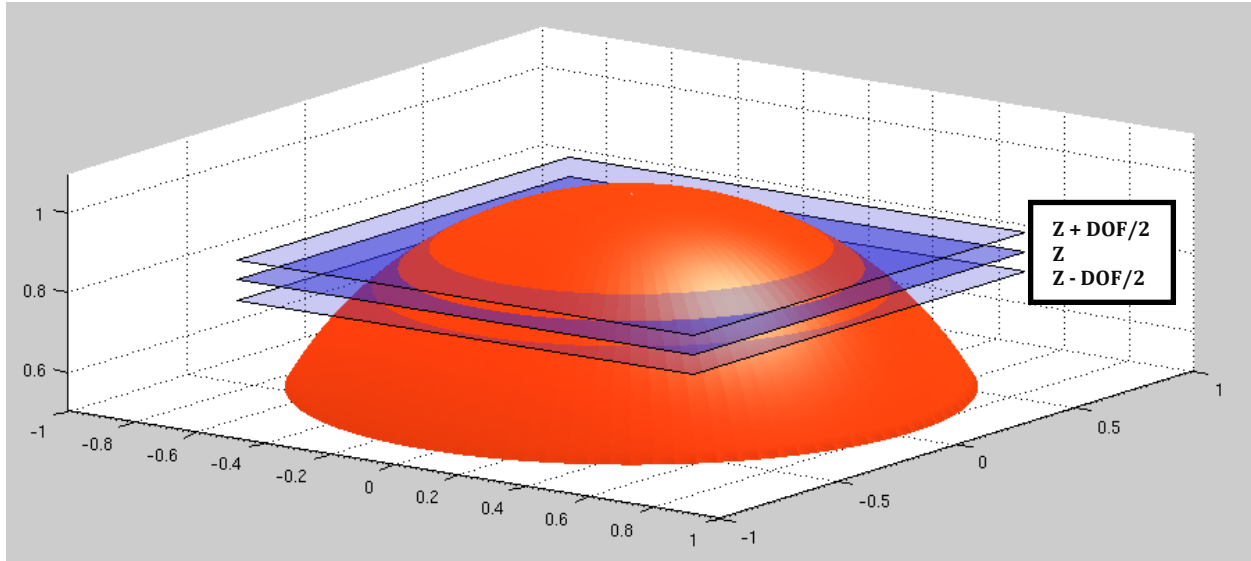
Figure 2. Optical sectioning properties of a confocal microscope. Above: The intersection of the focal plane and a spherical sample. The focal plane, located at Z, is shown in dark blue, and the two light blue planes above and below represent the planes at plus and minus one half of the depth of field (DOF). Left: The simulated intensity pattern measured at focus position Z. The peak intensity occurs at Z, and has diminished to near zero at Z + DOF/2 or Z – DOF/2. This image is referred to as an optical section because it represents a cross section of the sample.

Surface profile information can be obtained by collecting multiple optical sections at different sample-objective lens distances (Z). To understand how this produces surface profile information, consider the intensity measured as a function of Z at a single object point. By stepping Z—either by moving the sample or the microscope objective lens—and recording intensity at each Z position, the axial response of the system will be measured. Performing such a scan on a perfect plane produces the impulse response of the system, also known as the axial point spread function (PSF). It can be shown that in the case of both perfectly reflecting and highly scattering objects, the maximum intensity of the axial PSF

coincides with the Z position of the sample surface [5], making confocal surface profiling ideal for irregular objects as well as smooth ones. It is assumed that the axial point spread function is spatial frequency band-limited, so the Nyquist-Shannon sampling theorem may be applied in order to reconstruct the microscope's continuous axial response to a given sample in the object plane. This is done by acquiring optical sections with Z frequency at least equal to twice the highest spatial frequency in the axial PSF. It can be shown that the resulting measurement is the convolution of the geometric surface with the microscope axial PSF [6], so deconvolution algorithms can be used to compute the surface location with accuracy better than the Z step size. In the case of the Leica DCM3D, the surface is measured to one one-hundredth of the Z scan step size. Figure 3 shows an axial response measured on an ICF capsule using a 40x 0.5NA lens.

Intensity (arbitrary units)

Z (step number)
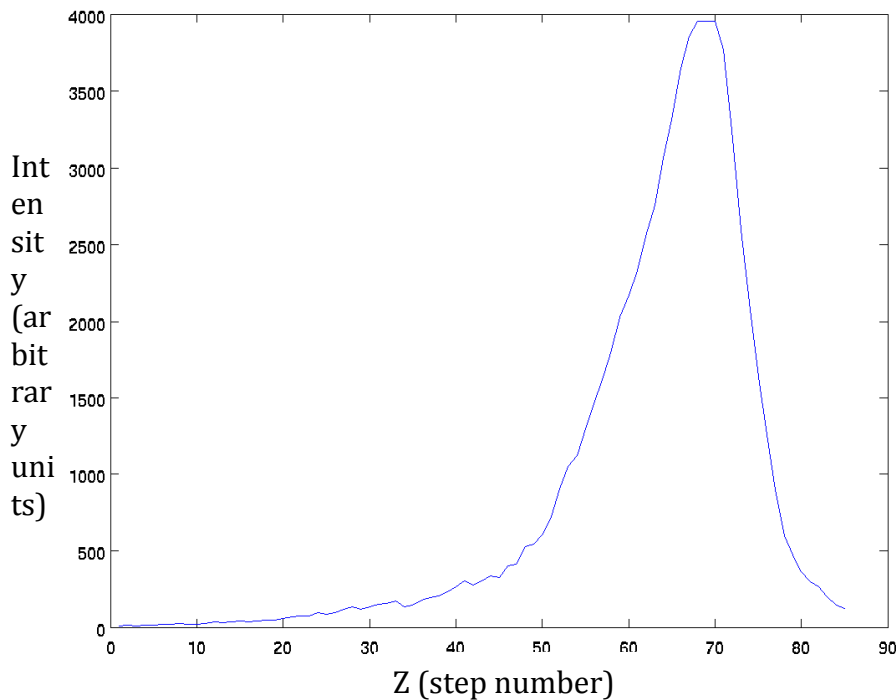
Figure 3. Axial PSF measured on an ICF capsule. The peak intensity corresponds to the image number at which the capsule is best in focus.

Once the topography data have been computed, an extended depth of field image can be produced by displaying the maximum intensity at each pixel. Figure 4 shows a damaged region of a capsule as seen by a standard light microscope (upper left), a single optical section produced by a confocal microscope (upper right), a confocal extended depth of field image (lower left), as well as the accompanying confocal surface profile data (lower right). In the standard light microscope and optical sections images, only a small annular zone of the capsule is in focus—between Z-DOF/2 and Z+DOF/2— which prevents analysis of the entire field of view in a single image. However, the extended depth of field image is fully in focus across the entire field, making analysis of the field of view possible from a single

image. Additionally, the extended depth of field image benefits from increased lateral resolution and reduced stray light when compared to bright field [6]. The height data clearly show the spherical shape of the capsule, as well as depressions where the capsule has been damaged.
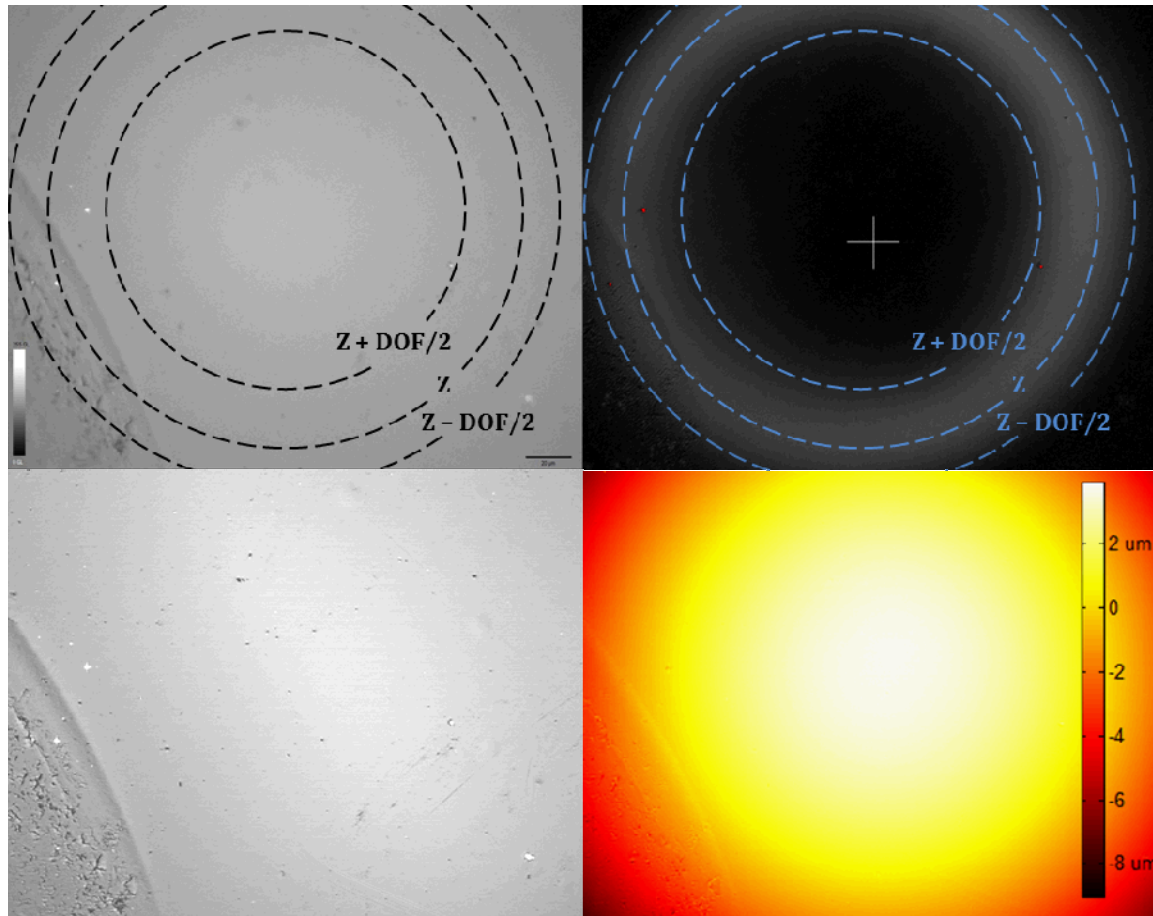
Figure 4. Standard bright field image of surface damage on an ICF capsule with in-focus region marked in black (upper left); a confocal optical section at a fixed Z position with in-focus optical section marked in blue (upper right); a confocal extended depth of field image (lower left); topographic data computed from focus scan (lower right)

After a full range of testing and market surveys, the Leica DCM3D, an integrated confocal microscope and interferometer, was selected because of its ability to measure objects spanning an extremely broad range of roughness, including highly irregular particles and the very smooth surfaces of capsules. The software provided with the system automatically fits the axial PSF to the acquired Z scan data at each pixel in the field of view, providing a single image file containing a uniform grid of pixels, each of which has both the peak reflectivity and computed height values. Leica also provide a full suite of remote control commands, facilitating full automation of the data acquisition process.

It was found during preliminary testing that the Leica DCM 3D produced viable height data only under magnifications of 100x or greater. Each 100x image provides a field of view of

120 μm by 90 μm with a pixel size of .166 μm and vertical resolution of 10 nm. Each high magnification image takes between 1 and 10 minutes to acquire, depending on the location on the capsule. Complete coverage of the surface at 100x requires approximately 2000 images, which results in acquisition times on the order of 2 days. Though slow to acquire, these high magnification images contain sufficient lateral and vertical precision to meet the requirements set forth for the CFTA mapping system. Figure 5 shows the Leica DCM 3D microscope itself and an example of the data provided by the DCM3D from a high magnification scan.
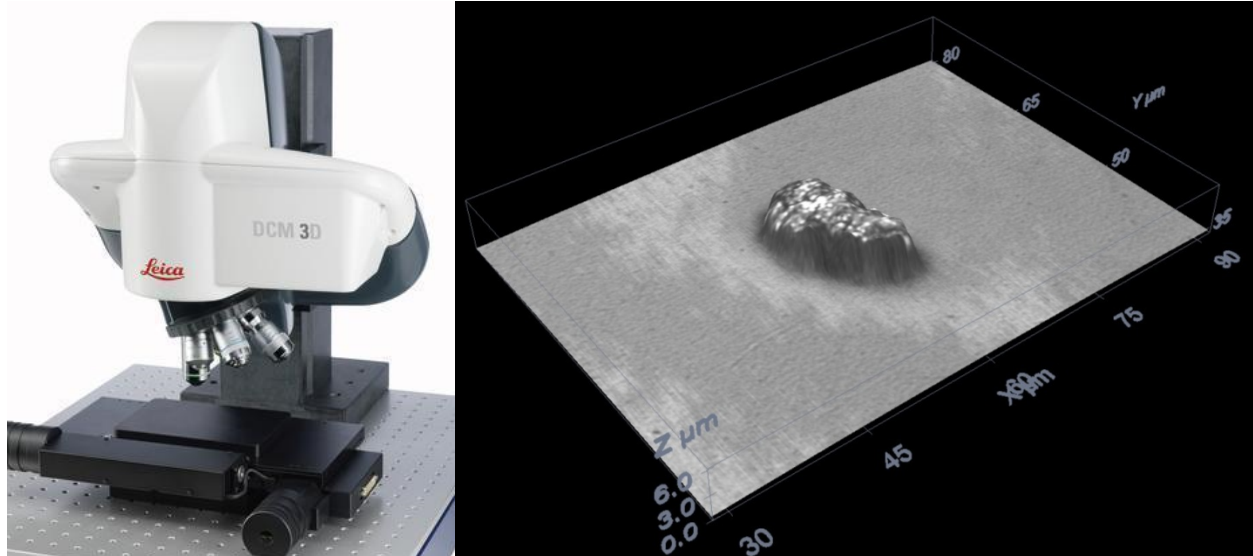

Figure 5. The Leica DCM 3D microscope system (left) and an isometric rendering of a surface profile measurement of a large particle using a 100x 0.9 NA objective lens. The intensity data are mapped onto the rendered height data for visualization purposes.

3.3 Capsule surface mapping overview

The CFTA Mapping System consists of a combination of the Leica DCM 3D confocal surface profiling microscope with integrated focus motor affixed to a nine-axis custom-built Aerotech linear positioner system. Two vacuum chucks—typically referred to as "wands"— with diamond-turned surfaces are used to handle the CFTA. The primary wand is used for inspecting the majority of the surface, and the secondary wand is used for inspecting the region initially obscured by the primary wand. Figure 6 shows a line drawing of the CFTA mapping system with the axes and wands labeled.
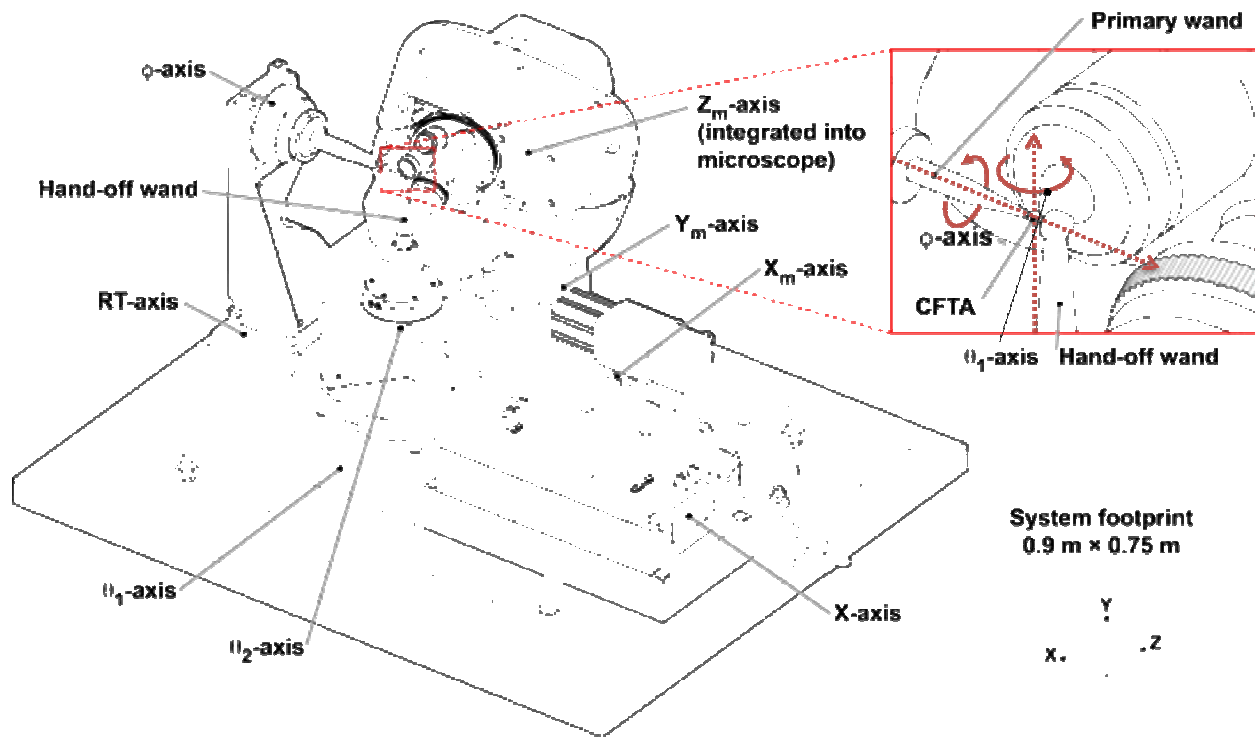
Figure 6. Line drawing of the completed CFTA mapping system with all 10 axesand the primary and secondary ("Hand-off") wands labeled.

Though the system precision requirements demanded high magnification images using 100x or greater, the small field of view and long scan times lead to prohibitively long measurement times when inspecting an entire capsule. In an early test it was shown that mapping an entire capsule using 100x magnification took approximately two and a half days. However, when using a 50x lens to acquire an initial map of the capsule, high magnification only needed to be acquired for a small number of specific objects. This so called "hit-list" method greatly reduced the inspection time, allowing complete capsule mapping in as little as ten hours.

In order to implement the hit-list method, the capsule is first mapped using a 50x long working distance lens with numerical aperture of 0.55. Once the CFTA is loaded into the primary inspection vacuum wand, the wand and CFTA are affixed to a vacuum base on φ-axis [2]. By rotating the φ and θ_1 axes, an array of low magnification confocal datasets are acquired that cover the exposed surface area of the capsule. Figure 7 shows the pattern used to acquire the images, as well as a sample dataset displayed on a sphere [4]. As each image is acquired, it is uploaded to a remote image processing system that identifies any features within the image. Once the complete group of images have been acquired and processed, a global, priority-ranked list of features and their locations is calculated. Individual high magnification scans are then acquired using a 100x lens with numerical aperture of 0.9, providing quantitative topography of each object of interest. Once the primary region of the capsule has been measured, the CFTA is transferred to the secondary wand so that the previously obscured region can be mapped using a 100x 0.75 numerical aperture lens. This process is described in more detail in section 3.4.
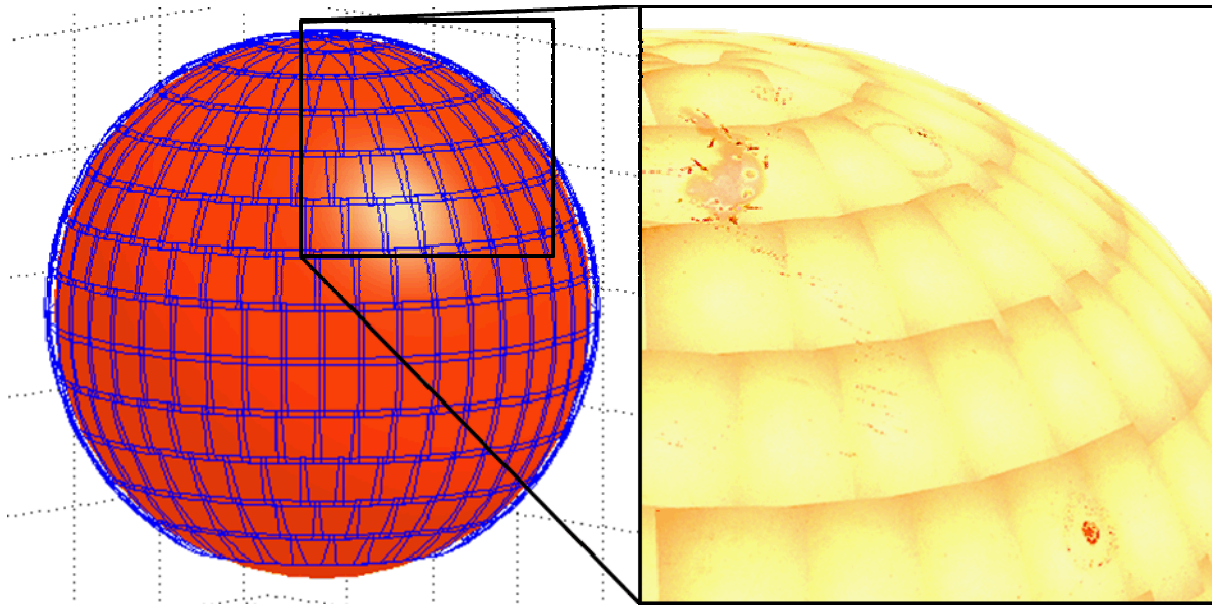
Figure 7. The low magnification image pattern used to cover 90% of the capsule surface (left). Therectangular outlines each represent the location of an individual image.The bare region on the bottom of the capsule represents the surface area that is obscured by the primary inspection wand. On the right is a region of actual data set rendered on a sphere for visualization purposes.This view allows qualitative assessment of defects and scratches that span multiple images.

3.4 The positioning system

Manipulating the CFTA such that the entire surface area can be safely positioned under the microscope is done using a 9-axis stage system that utilizes Aerotech Inc. Nanopositioner stages. Additionally, the microscope contains a closed-loop, high precision focus motor, giving the system a total of 10 motion axes; all axes are labeled in Figure 6. The $\square$ and θ_1 axes are used rotate the wand and capsule during primary mapping, while the RT, X_m and Y_m axes are used to compensate for wand and capsule variation as the rotation axes move. This allows access to 90 percent of the capsule surface, but the primary wand obscures about 10 percent of the capsule surface area, necessitating the use of another wand [1].

In order to view the wand-obscured region, the capsule is handed-off to the secondary wand. Once the capsule is handed off, the primary wand is retracted using the R axis, exposing the fill tube (Figure 8). Then, the secondary wand and capsule are rotated about the θ_1 axis using the θ_2 motor while the θ_1 motor is used to rotate the primary wand about the same axis, keeping the fill tube straight (Figure 9). Due to mechanical interference between the primary wand and the microscope, the capsule can only be rotated 10 degrees using this method. However, a total rotation of 90 degrees is required in order to expose the wand-obscured region to the optics. To complete the remaining 80 degrees of rotation, the capsule and secondary wand are rotated through the remaining 80 degrees while the R and T stages move in synchrony with the θ_2 axis in such a way that the fill tube neither tensioned nor compressed (Figure 10). This complex motion has been developed such that

it minimizes stress and strain in the fill tube, maximizing the probability that both the fill tube and the fill tube-to-capsule glue joint survive the maneuver.

Once the capsule has been rotated, the region previously obscured by the primary wand is facing the microscope, and high magnification data are then acquired in a uniform XY grid pattern using the XM, YM, and ZM motion axes (Figure 11). A low magnification scan is not acquired in this region due to optical limitations of the microscope. Because all images are high magnification, the topography data from these images are immediately evaluated in the same manner as the high magnification images acquired on the primary region of the capsule. This step completes measurement of the entire capsule surface. The fill tube is then unbent and returned to the primary wand for immediate installation into the final target assembly.
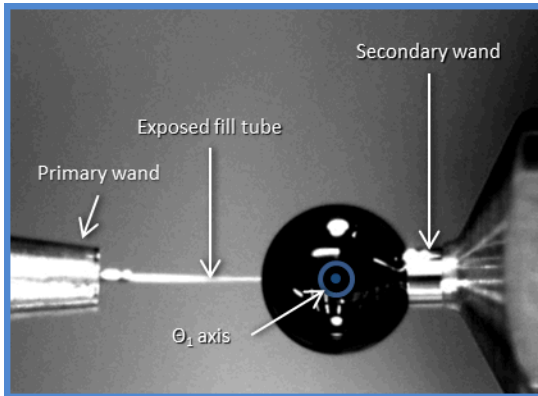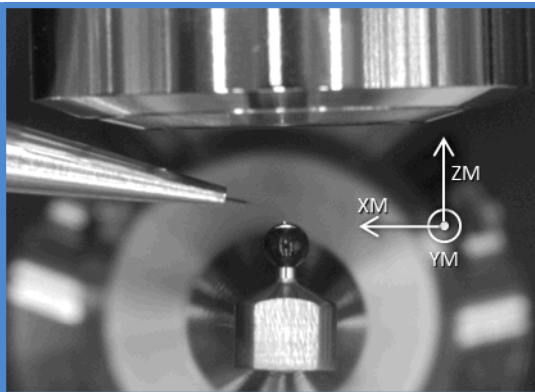

Figure 8 : CFTA after transfer to secondary wand and retraction of primary wand along R axis

Figure 9 : θ_1 and θ_2 rotated about θ_1 axis
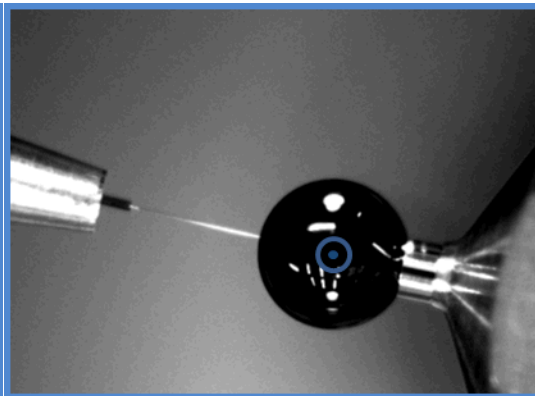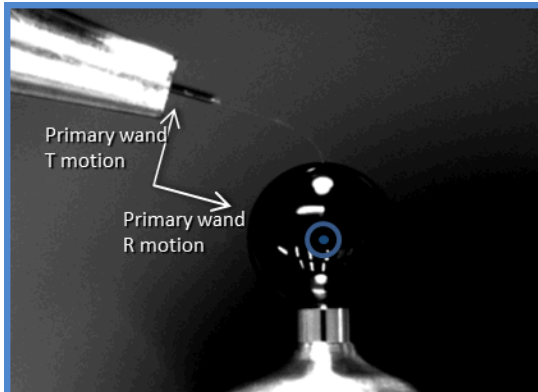
Figure 10 : As θ_2 is rotated, the primary wand is translated along the R and T axes, minimizing stress during the maneuver

Figure 11 : Remaining surface area inspected using 100x 0.75NA long working distance lens. The capsule is held stationary and the microscope translated using XM, YM, and ZM

3.5 The automated acquisition system

In order to cover the entire surface of a standard capsule, hundreds of scans must be performed, taking anywhere from twenty seconds to 10 minutes each, depending on magnification and location on the CFTA. Because of the large volume of individual measurements, automated acquisition code was required. A fully automated calibration and acquisition system has been developed using a combination of the AeroBasic, the Aerotech automation language, and LabVIEW.

The acquisition system contains many features that maximize flexibility and minimize inspection time. In order to increase flexibility and relax manufacturing tolerances for the primary and secondary inspection wands, the acquisition system includes algorithms to automatically align and calibrate individual inspection wands each time a measurement is performed. Once calibration is complete, the system begins acquiring data. Because of the large quantity of images needed to cover the entire surface, each image is analyzed immediately after it is acquired.

Once all low magnification images have been analyzed, a global list of detections is generated. Due to overlap between each image with up to four neighbors, a single individual object on the capsule surface can result in up to five individual detections. Thus, if a high magnification image is taken at of every detection location, one object could be counted multiple times, resulting in an artificially high defect count. Additionally, if multiple objects are close together, they will fall within a single high magnification field of view which can also cause over counting.

Figure 12 shows an example of how these issues can lead to significant over counting of the total number of defects. The low magnification image borders are outlined with solid blue, and each individual detection is outlined in dashed red. This set of images contains only two real objects, numbered 1 and 2. However, object 1 is split between four different images, resulting in four detections of the same object. Additionally, objects 1 and 2 are close enough that an image centered on object 1 would contain object 2, and an image centered at object 2 would contain object 1. In this example, taking a single image at the location of each of the five individual detections would lead to five separate images, each containing the same two defects. The total defect count would then be 10, when in reality there are only two objects. This would lead to erroneous failure of capsules when compared against the defect allowance outlined previously.

In order to combat the over counting issue, an algorithm has been developed that prevents over-counts due to both clusters and image overlap. First, clusters of detections that fall within a specific distance of each other are identified and grouped. Then, the area-weighted center of mass of the cluster is calculated. By calculating a bounding box with dimensions equal to the high magnification field of view, and centering the bounding box at the cluster center of mass, the list of detections falling within a high magnification image taken at that location can be calculated. Those detections are then removed from the detection list, and the process repeated until all detections above a specified size have been included in at least one high magnification bounding box.

For the example shown in Figure 12, the algorithm produces only one high magnification image coordinate—the bounding box is shown with the green dotted lines—that will include both objects in a single image. This approach is known to be susceptible to duplicate objects in the extreme edges of the field of view. However, because the cluster center of mass is usually biased toward the largest objects, the double counts occur for the smallest objects, decreasing their impact on the final defect count. Ultimately, a high magnification duplicate removing algorithm must be employed to eliminate *all* over-counting, but the low magnification approach has never produced an over-count on an object greater than 7.5 µm^3 since its deployment.
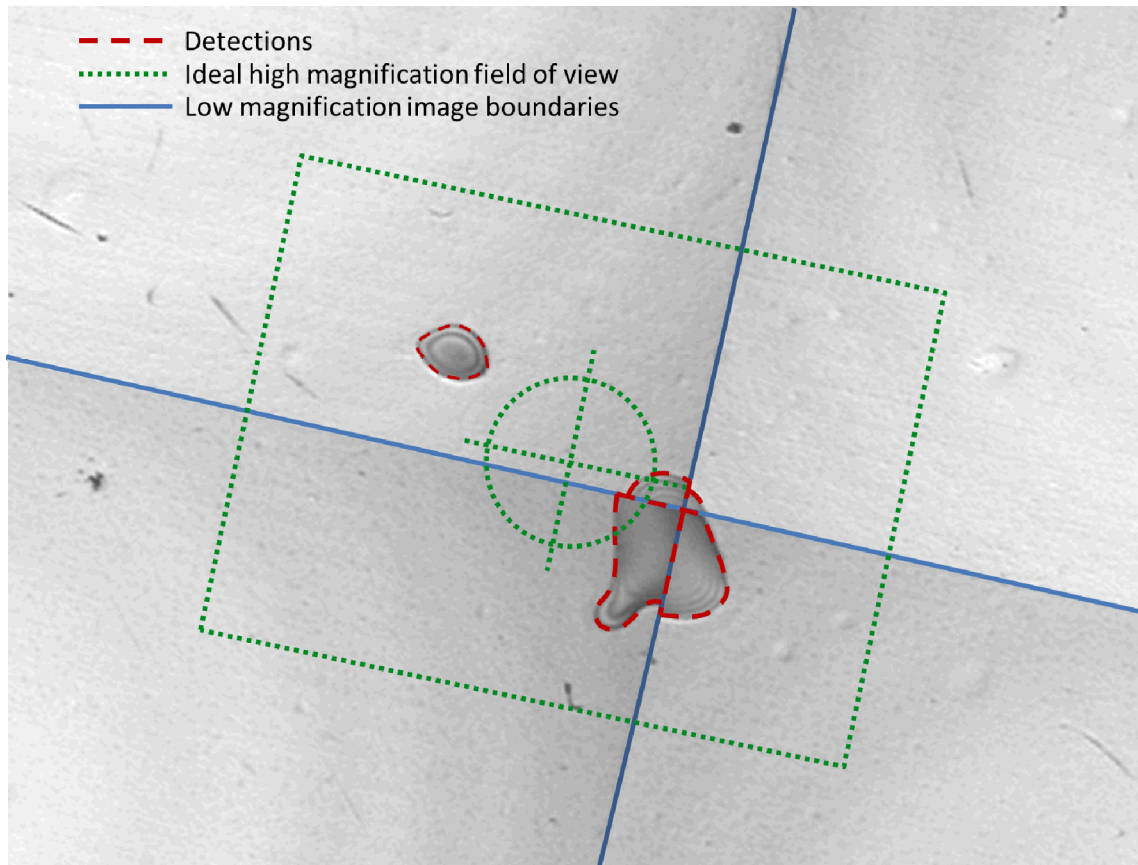

Figure 12. Example low magnification detections that could lead to over counting in high magnification. Low magnification detections are outlined with red dashes, the image boundaries are the blue solid lines, and the ideal single high magnification image placement is illustrated with green dotted lines.

3.6 The image processing and data management system

Feature identification within each image is done using a local area signal-to-noise ratio (LASNR) image segmentation algorithm.[3] This algorithm is applied to the intensity information within the low magnification data when generating the global defect list. The topography data from the high magnification images are analyzed using LASNR, providing volume measurements of individual features. Figure 13 demonstrates an example of

features as measured and analyzed in both low magnification intensity and high magnification topography. The results of the image segmentation are stored in a relational database, facilitating future analysis.
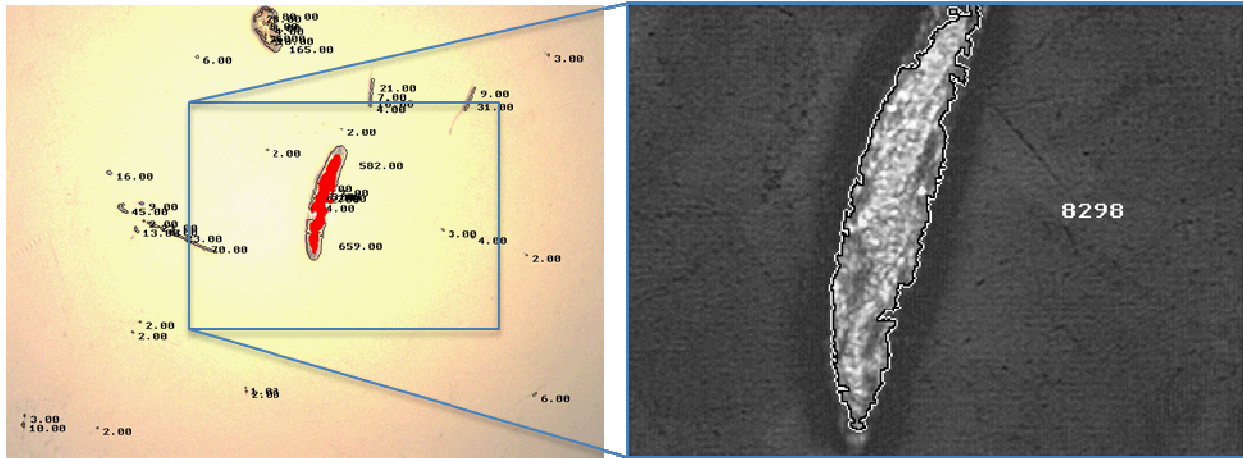
Figure 13. Left - Defect located using the LASNR algorithm. The black overlay shows the boundaries of the isolated defects and their areas in pixels. Red represents poorly computed height data, which is common in low magnification scans. LASNR performs well even when there are a large number of dropped pixels Right – LASNR segmentation applied to topography data from a high magnification scan. The white number is the measured volume of the large particle in μm^3, and the black-and-white line is the particle boundary.

4. Conclusion

A fully automated system for topographic characterization of surface features on ignition target capsule surfaces has been described. This CFTA Mapping System is able to volumetrically quantify isolated features of sizes 7.5 μm^3 and larger with an accuracy of ± 10 percent with a positional accuracy is better than 0.25 degree across the entire capsule surface. This is accomplished using a surface profiling confocal microscope, a 9-axis high precision positioning system, and a full suite of automated acquisition and processing code. Due to the high degree of automation, the system is able to keep up with the throughput demands of ICF targets, assuring the characterization of capsules for ignition experiments and providing vital data needed understanding Rayleigh-Taylor instability during implosion due to surface anomalies on capsule ablators.

References

1. http://meetings.aps.org/link/BAPS.2010.DPP.TO5.5
2. Buice, E.S. et. al, 2011, "3D Surface Mapping of Capsule Fill-Tube Assemblies used in Laser-Driven Fusion Targets," European Society for Precision Engineering and Nanotechnology Como, Italy, May 23, 2011 through May 27, 2011
3. Kegelmeyer, L. M., Fong, P., Glenn, S. M., and Liebman, J., 2007, "Local Area Signal-to-Noise Ratio (LASNR) algorithm for Image Segmentation," Proc. SPIE 6696, 66962H (2007).
4. D. Potter, N. Antipa, Visualization of Target Inspection data at the National Ignition Facility,

5. R.C. Montesanti, M.A Johnson, E.R. Mapoles, D.P. Atkinson, J.D. Hughes, J.L. Reynolds. Phase-Shifting Diffraction Interferometer for Inspecting NIF Ignition-Target Shells. In *Proceedings of the American Society for Precision Engineering 2006 Annual Meeting*, 2006.
6. Wilson, T. "Confocal Microscopy." *Confocal Microscopy.* San Diego: Academic Press Inc., 1990.